Simultaneous blastic plasmacytoid dendritic cell neoplasm and myelofibrosis: A case report

FUYI LUO[1,2], BINGJIE LI[3], JING LI[4] and YAN LI[2]

[1]Graduate School, Hebei North University, Zhangjiakou, Hebei 075000;
Departments of [2]Hematology and [3]Pathology, Hebei General Hospital; [4]Department of Hematology,
Hebei Province Hospital of Chinese Medicine, Shijiazhuang, Hebei 050000, P.R. China

Received August 2, 2023; Accepted December 5, 2023

DOI: 10.3892/ol.2024.14354

Abstract. Blastic plasmacytoid dendritic cell neoplasm (BPDCN) is an extremely rare and aggressive tumor with an unknown pathogenesis. Myelofibrosis (MF) is a type of myeloproliferative neoplasm. MF can be secondary to several hematological malignancies, including chronic myeloid leukemia, myelodysplastic syndrome and hairy cell leukemia. In the present report, a rare case of BPDCN secondary to MF is described. A 70-year-old male patient developed a large purplish-red rash with recurrent symptoms. BPDCN was confirmed by immunohistochemistry of a biopsy specimen and flow cytometry of bone marrow cells. Bone marrow histopathology revealed MF. Next-generation sequencing of peripheral blood revealed mutations in the Tet methylcytosine dioxygenase 2 and NRAS proto-oncogene GTPase genes. The patient underwent one cycle of chemoimmunotherapy, but the condition progressed, an infection developed and the patient eventually died. The present case suggests that BPDCN can occur in conjunction with MF and that the prognosis of such patients is poor. Pathological examination and genetic testing aided in the diagnosis and treatment. This case emphasizes the need to raise awareness of BPDCN among clinicians and to be alert to the potential for fatal infection in patients with BPDCN combined with MF following myelosuppression triggered during chemotherapy.

Introduction

Blastic plasmacytoid dendritic cell neoplasm (BPDCN) is a rare and aggressive hematological malignancy with a mostly poor prognosis. In the United States, approximately 0.04 cases of BPDCN per 100,000 individuals have been reported between 2008 and 2014, with a median overall survival (OS) of 8-20 months (1). The condition tends to occur in older adults with a median age of 60-70 years and most individuals diagnosed with the disease are male (2). BPDCN originates from plasmacytoid dendritic cells, and its most common clinical manifestations are cutaneous lesions, bone marrow involvement and leukemic dissemination (3). $CD4^+$ and $CD56^+$ tumor cells are typical of BPDCN, and CD123, transcription factor 4 (TCF4), T cell leukemia/lymphoma protein 1 (TCL1), CD304 and CD303 (also referred to as blood dendritic cell antigen 2) are its main markers (4,5). BPDCN does not express typical markers of a lymphoid or myeloid lineage (6). There are no consensus treatment guidelines for BPDCN (7). Retrospective studies have demonstrated that regimens based on lymphoid leukemia are associated with improved remission rates compared with those based on myeloid leukemia or lymphoma (2,8). Regardless of the regimen, however, disease relapses are frequent and rapid (9,10). In addition, allogeneic stem cell transplantation (alloSCT) is the only known potential cure for BPDCN (3,11). The 5-year OS, disease-free survival, recurrence and non-recurrence mortality rates for patients with BPDCN who receive alloSCT are 51.2, 44.4, 32.2 and 23.3%, respectively (11).

Myelofibrosis (MF) is a type of myeloproliferative neoplasm (MPN), which is clinically characterized by progressive anemia, splenomegaly and systemic symptoms (including fatigue, night sweats and fever) (12). The pooled annual incidence rate of primary myelofibrosis (PMF) in Europe, North America and Oceania between 1946 and 2012 was 0.47/100,000 (13). The five independent risk factors in the International Prognostic Scoring System for PMF include age >65 years, hemoglobin <10 g/dl, white blood cell count $>25x10^9$/l, circulating blasts ≥1% and presence of constitutional symptoms (14). Based on these variables, PMF is categorized into four groups: Low-risk, intermediate-risk-1, intermediate-risk-2 and high-risk, corresponding to a median OS of 11.3, 7.9, 4 and 2.3 years, respectively (14). Treatment of PMF requires individualized assessment based on the spleen size, symptom burden and risk stratification (15). Most current pharmacologic treatments for PMF are palliative in scope, such as Janus kinase 2 (JAK2) inhibitors (ruxolitinib) (12). The overall mortality rates before and after ruxolitinib approval

Correspondence to: Professor Yan Li, Department of Hematology, Hebei General Hospital, 348 Heping West Road, Xinhua, Shijiazhuang, Hebei 050000, P.R. China
E-mail: 18931866300@163.com

Key words: blastic plasmacytoid dendritic cell neoplasm, myelofibrosis, TET2 gene mutation, NRAS gene mutation, DNA methylation, MAPK pathway

were 79.8 and 47.3%, respectively, and the overall risk of death was reduced by 53% with ruxolitinib approval (16). MF can be secondary to several hematological malignancies, including chronic myeloid leukemia, myelodysplastic syndrome and hairy cell leukemia (17-19).

The present study reports the case of an elderly male patient with BPDCN in combination with MF. Among previous studies, only one case report was found on the conversion of PMF to BPDCN (20); however, to the best of our knowledge, there is no relevant literature on MF secondary to BPDCN. The case is unique as the patient was $CD4^-$, with combined MF and mutations in the Tet methylcytosine dioxygenase 2 (TET2) and NRAS proto-oncogene GTPase (NRAS) genes, which is rare. Future research is required to further elucidate the potential relationship between these two different diseases.

Case report

Case. In May 2021, a 70-year-old male patient gradually developed a large, dark, purplish-red rash on the chest, abdomen and upper back without concomitant symptoms, such as itching, pain or fever, following a vaccination against severe acute respiratory syndrome coronavirus 2. The patient said that they went to the Dermatology Department of the Fourth Hospital of Hebei Medical University (Shijiazhuang, China), and were treated with oral antiallergic medication for 2 months (details unknown), after which their skin returned to normal. In September 2021, the patient went to Shijiazhuang People's Hospital (Shijiazhuang, China), for incomplete intestinal obstruction, and on the third day of hospitalization, a rash reappeared without any apparent trigger and was more severe than the previous one. The patient was given dexamethasone (5 mg intramuscular QD), ebastine (20 mg oral QD), benadryl (20 mg intramuscular QD) and topical glycerite lotion, and the rash symptomatically improved after 4 consecutive days of medication. During hospitalization, whole body CT was examined, and there were multiple enlarged lymph nodes in the abdominal cavity and retroperitoneum (details unknown). In April 2022, the patient developed symptoms of generalized malaise, and went to Shijiazhuang Hospital of Traditional Chinese Medicine (Shijiazhuang, China), and the repeat whole body CT suggested that the number of enlarged lymph nodes in the abdominal cavity had increased compared with the previous one, and the patient did not receive any treatment. However, the condition was recurrent and gradually worsened. In May 2022, the patient was admitted to Hebei General Hospital (Shijiazhuang, China) (Fig. 1A). A physical assessment revealed the following: Temperature, 36.3˚C (normal range, 36.1-37.0˚C); pulse, 88 beats/min (normal range, 60-100 beats/min); respiration, 22 breaths/min (normal range, 16-20 breaths/min); blood pressure, 112/69 mmHg (normal range, 90-130/60-80 mmHg); conscious; no jaundice. Skin and mucosal examinations revealed a large, dark, purplish-red rash on the chest, back (Fig. 1B and C) and left inner thigh. A lymph node assessment showed palpable enlarged lymph nodes on the left supraclavicular region, which were tough and could be pushed without pressure pain, while the remaining superficial lymph nodes were not enlarged. An abdominal examination revealed no evidence of hepatosplenomegaly. Other findings were unremarkable. The patient had a previous history of hypertension for 10 years, regular administration of amlodipine besylate, well-controlled blood pressure, and no other medical history, including hematological neoplasms.

Laboratory assessment results at admission and after one course of VA regimen (venetoclax 100 mg, D1; 200 mg, D2-28; azacytidine 0.1 g subcutaneously, D1-7) are presented in Table I. White blood cells, lymphocytes, cytokines interleukin (IL)-6 and IL-10 markedly decreased after treatment compared with before, but C-reactive protein levels were increased. Next-generation sequencing of peripheral blood, which assessed the protein-coding regions of 267 genes strongly associated with hematological disorders, revealed multiple mutations, including exosome complex exonuclease RRP44 (DIS3; 13q22.1), NRAS (1p13.2), TET2 (4q24), CUB and Sushi multiple domains 1 (CSMD1; 8p23.2), B-cell lymphoma (BCL)6 corepressor-like protein 1 (Xq26.1) and platelet-derived growth factor receptor (PDGFR)A (4q12) mutations (Table II). However, no mutations were found in the FMS-related receptor tyrosine kinase 3 (FLT3), JAK2, STAT, calreticulin (CALR) or MPL proto-oncogene thrombopoietin receptor (MPL) genes. Bone marrow cell classification showed that the proportion of lymphocytes was notably increased, and atypical lymphocytes were easily seen (73.5%) (Fig. 2A). Bone marrow tissue biopsies showed highly active myelodysplasia (60-70%) and reticular fiber staining was grade 2 (Fig. 2B-T) (21). Immunohistochemistry of cutaneous, lymph node and bone marrow tissue biopsies supported a diagnosis of a BPDCN (Figs. 1F-K, 2 and 3). Immunohistochemical examination of the bone marrow and lymph nodes was positive for TET2, NF-κB, NRAS and phospho (p)-ERK, and negative for PDGFRA, IL-6, IL-10, JAK2, STAT3 and TGF-β1. Flow cytometry analysis of the bone marrow showed abnormal cells, with 54.61% (Fig. S1B) expressing CD56 (Fig. S1K), CD45RA (Fig. S2A), CD2 (Fig. S2B), CD303 (Fig. S3D), human leukocyte antigen DR (Fig. S3E) and CD36 (Fig. S4B), partially expressing CD4 (Fig. S2C), CD103 (Fig. S2D), CD10 (Fig. S2E) and CD123 (Fig. S4A), weakly expressing CD7 (Fig. S2F), TCL1 (Fig. S4C) and T-cell restricted intracellular antigen 1 (Fig. S4D), and lacking expression of other myeloid or lymphoid markers. Additional detailed results of flow cytometry are shown in Figs. S1-7. CT demonstrated multiple enlarged lymph nodes above and below the transverse septum and splenomegaly with slight hypermetabolism. The largest retroperitoneal para-abdominal aortic lymph node was 30x20 mm (Fig. 4A, C and E). On the basis of these findings, the patient was diagnosed with BPDCN complicated by MF. The patient received a course of VA regimen (venetoclax 100 mg, D1; 200 mg, D2-28; azacytidine 0.1 g subcutaneously, D1-7). On day 6 of chemotherapy, the skin lesions had almost subsided (Fig. 1D and E) and the lymphocyte count had gradually decreased during this treatment period (Table III). On day 10 of chemotherapy, the patient was discharged.

The second day after the first course of chemotherapy, the patient was admitted to the hospital again and the laboratory assessment results at readmission are shown in Table I. The patient presented with granulocyte deficiency with a fever, and CT demonstrated splenomegaly, ascites and multiple lymph nodes that had increased and enlarged, with few lymph nodes that were smaller than before (Fig. 4B, D and F). This indicated

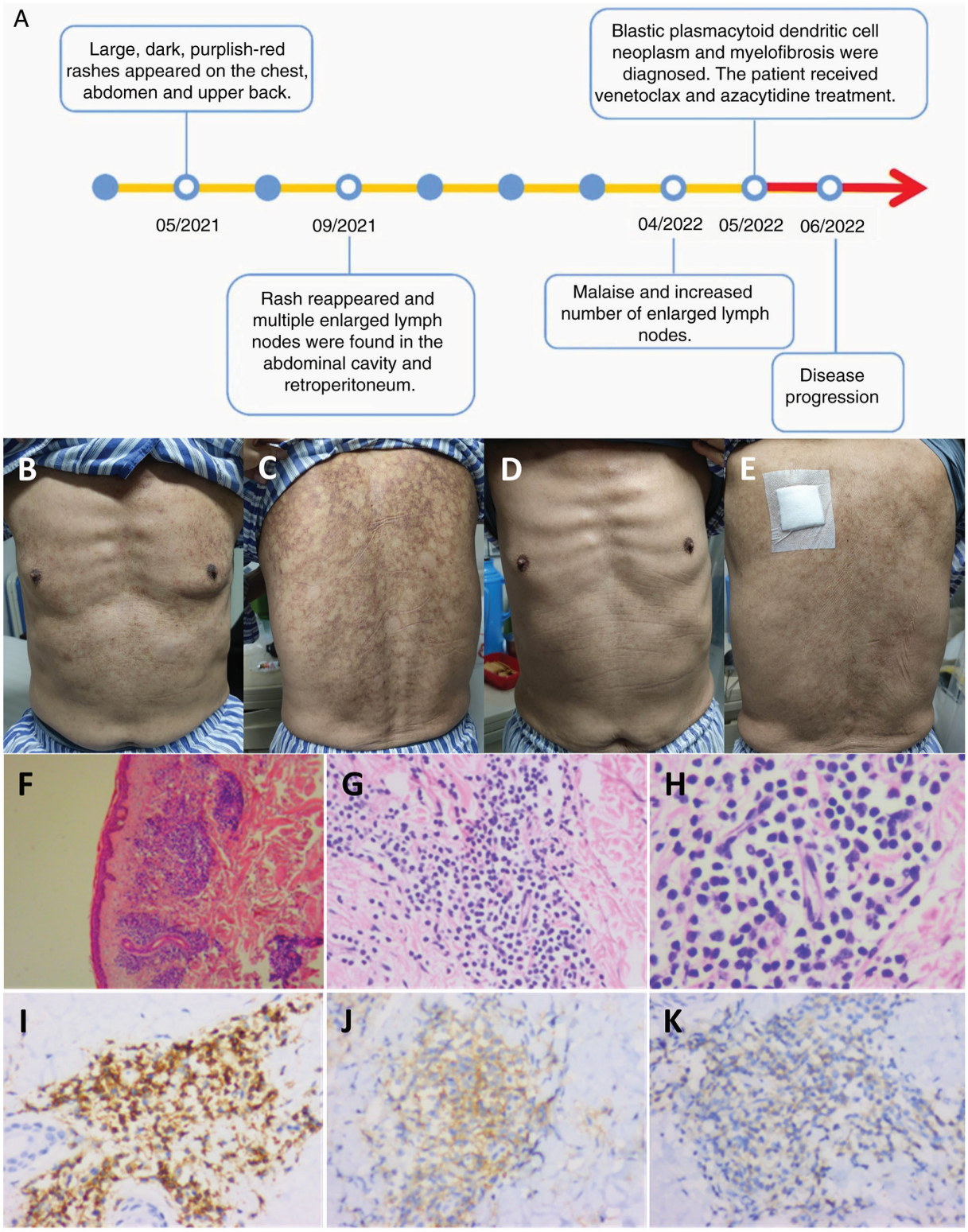

Figure 1. Timeline, images and pathology of the skin. (A) Timeline of disease progression. (B-E) Skin rashes on the (B) chest and (C) back before treatment and on the (D) chest and (E) back after 6 days of chemotherapy. Pathological findings of the skin rashes, visualized using hematoxylin and eosin staining at (F) x40, (G) x200 and (H) x400 magnification. (I) $CD43^+$ (magnification, x200), (J) $CD56^+$ (magnification, x200) and (K) $CD123^+$ (magnification, x200) immunohistochemistry staining results. No obvious lesions were seen in the epidermis, but a large number of blastoid cells had infiltrated around small blood vessels in the dermis and skin appendages, which were single in morphology and medium in size, with round or oval nuclei, fine-grained chromatin and a small nucleolus.

that the effect of the treatment was poor. Subsequently, the condition of the patient progressed and included respiratory failure, acute renal injury and delirium. A series of treatments were administered, such as anti-infection medication [meropenem, 1 g intravenous (IV), 5 days] and a red blood transfusion (recombinant human thrombopoietin, 1.5 WU, subcutaneous, 2 days; human albumin, 20 g IV, 1 time; human fibrinogen, 4 g IV, 1 time; leukocyte-depleted frozen plasma,

Table I. Laboratory findings.

Parameter	On admission	Second day after the first course of chemotherapy	Normal range/limit
Complete blood count			
White blood cells, 10^9/l	10.53	2.33	3.50-9.50
Neutrophils, 10^9/l	1.81	2.02	1.80-6.30
Lymphocytes, 10^9/l	7.60	0.24	1.10-3.20
Eosinophils, 10^9/l	1.60	0.00	0.02-0.52
Red blood cells, 10^{12}/l	3.10	3.10	3.80-5.10
Hemoglobin, g/l	91.00	92.00	115.00-150.00
Platelets, 10^9/l	70.00	104.00	125.00-350.00
C-reactive protein, mg/l	31.19	61.83	0.00-6.00
Coagulation			
Fibrinogen, g/l	3.14	0.69	2.00-4.00
D-dimer, mg/l FEU	1.65	5.12	0.00-0.55
β2-microglobulin, μg/ml	6.29	Untested	0.90-2.70
Biochemistry			
Total protein, g/l	59.30	67.40	65.00-85.00
Alanine transaminase, U/l	11.20	12.80	9.00-50.00
Aspartate transaminase, U/l	16.30	17.40	15.00-40.00
Alkaline phosphatase, U/l	78.50	138.30	45.00-125.00
Blood urea nitrogen, mmol/l	6.50	7.40	3.60-9.50
Serum creatinine, μmol/l	90.60	118.30	57.00-111.00
Uric acid, μmol/l	407.40	297.50	208.00-428.00
Glomerular filtration rate, ml/min	73.24	53.00	
Lactate dehydrogenase, U/l	259.10	203.00	120.00-250.00
Immunoglobulin			
IgG, g/l	11.69	Untested	8.60-17.40
IgA, g/l	1.26	Untested	1.00-4.20
IgM, g/l	0.63	Untested	0.50-2.80
Cytokine			
IL-6, pg/ml	47.51	13.92	0.00-5.30
IL-10, pg/ml	98.43	2.42	0-4.91
Vascular endothelial growth factor, pg/ml	55.39	Untested	0-142.20
Serum amyloid A, mg/l	87.22	233.46	<10.00
Procalcitonin, ng/ml	0.25	2.04	<0.06

FEU, fibrinogen equivalent units; Ig, immunoglobulin; IL interleukin.

400 ml IV, 1 time). An intermittent fever persisted; however, the neutrophil count on day 5 after the first course of treatment was slightly low and the rest of the neutrophil counts after the first course of chemotherapy were within the normal range (Table III), no causative organisms were detected in the sputum, blood or urine, and no lung infection was seen on the chest CT. The site of infection could not be determined and the condition of the patient continued to progress. The general condition of the patient was so poor that the next course of chemotherapy was not administered. Finally, the patient requested to be discharged from the hospital due to financial reasons. In July 2022, a follow-up phone call established that the patient had died.

Next-generation sequencing of peripheral blood

Wet experiment part. Nucleic acid extraction was performed using the Blood Genomic DNA Extraction Kit (0.1-1 ml; cat. no. YDP348-03; Tiangen Biotech Co., Ltd.). Nucleic acid quality inspection was performed using a NANODROP ONE (Thermo Fisher Scientific, Inc.) to measure the preliminary DNA concentration, A260/280 and A260/230, where A260 is the absorption wavelength of the highest absorption peak of nucleic acid and A280 is the absorption wavelength of the highest absorption peak of protein. A230 is the absorption wavelength of the highest absorption peak of carbohydrates. A260/280 and A260/230 are indicative values of nucleic acid purity. An A260/280 ratio of 1.8-2.0 and an A260/230 ratio

Table II. Next-generation sequencing of the patient's peripheral blood.

Mutant gene	Chromosome	Mutation location, exon	Nucleotide alteration	Amino acid alteration	dbSNP reference no.	Mutation frequency	Sequencing depth, X
DIS3	13q22.1	17	c.2339G>C	p.R780T	-	0.166	1,661
NRAS	1p13.2	4	c.436G>A	p.A146T	-	0.045	1,474
NRAS	1p13.2	2	c.35G>A	p.G12D	rs121913237	0.017	2,051
NRAS	1p13.2	2	c.34G>A	p.G12S	rs121913250	0.035	2,044
TET2	4q24	3	c.2245C>T	p.Q749*	-	0.011	1,881
TET2	4q24	5	c.3578G>A	p.C1193Y	-	0.580	1,573
TET2	4q24	11	c.4794T>G	p.Y1598*	-	0.182	1,994
CSMD1	8p23.2	14	c.2012G>A	p.R671H	rs376413480	0.137	1,576
TET2	4q24	9	c.4160A>G	p.N1387S	-	0.039	1,272
BCORL1	Xq26.1	4	c.469G>A	p.A157T	rs147775035	0.998	996
PDGFRA	4q12	15	c.2153G>A	p.R718Q	rs367722824	0.667	1,443

dbSNP, Single Nucleotide Polymorphism Database; DIS3, exosome complex exonuclease RRP44; NRAS, NRAS proto-oncogene GTPase ; TET2, Tet methylcytosine dioxygenase 2; CSMD1, CUB and sushi multiple domains 1; BCORL1, B-cell lymphoma 6 corepressor-like protein 1; PDGFRA, platelet-derived growth factor receptor A.

of 2.0-2.2 indicate that the purity of DNA is good. Qubit 4.0 fluorometer (Q33238; Thermo Fisher Scientific, Inc.) detection was used as the standard for library construction input. Raw samples were analyzed by electrophoresis (2.5% agarose gels) using DNA marker (BM401-01; TransGen Biotech Co., Ltd.) to initially confirm DNA integrity. The DNA library was constructed with a commercial kit (cat. no. 20025524; Illumina DNA Prep with Enrichment) and the length of the library was set to 220 bp. Library quality control was performed using a Qubit 4.0 to detect the library concentration, and Agilent DNF-915 Reagent Kits (Agilent Technologies, Inc.) were used to perform fragment analysis quality control on the Agilent 5200 platform (Agilent Technologies, Inc.). The average fragments ranged between 330 and 390 bp [dilution conversion formula for the concentration of the library: 1.25 nm x average molar mass of bases (660) x average fragment length of library (330-390 bp)/10^6=0.27-0.32 ng/μl (0.4-0.48 nM)]. Hybridization was performed using the Nextera DNA Flex Pre-Enrichment Library Prep and Enrichment Reagents 96 samples, and targeted capture amplification of the target region was performed with probes manufactured by Tianjin Xiehe Bojing Medical Diagnostic Technology Co., Ltd. The sequencing platform was Illumina novaseq6000 (Illumina, Inc.) with the NovaSeq6000 S1 Reagents Kit v1.5 (300 cycles; cat. no. 20028318). The sequencing input protocol was as follows: Samples to be uploaded were prepared and their molar concentrations were calculated, then the libraries were denatured and samples were detected at a concentration of 250 pM (1.25 nM). The molarity was calculated as follows: (ng/μl x10^5)/[660 g/mol x average library size (bp)]=Molarity (nM). The sequencing protocol was paired-end 150 bp sequencing.

Next-generation sequencing analysis. The quality control process Fastp (22) (version 0.23.2; https://github.com/OpenGene/fastp) was applied for FASTQ data by removing the terminal adaptor sequences and low-quality reads from the raw data. Dragen (version 3.10.4; Illumina, Inc.), a local installation hardware-accelerated sequencing processing pipeline, was used to perform data alignment and mutation calling. The lower limit of detection for variant allele frequency was 0.5%, and then an in-house algorithm was used to review hotspot variants. The final candidate variants were all manually verified in the Integrative Genomics Viewer (23) (IGV; https://www.igv.org/). Copy number alterations were identified using CNVkit (24) (version 0.9.10; https://cnvkit.readthedocs.io/en/stable/) with default parameters. The insertion and deletion caller Pindel (25) (version v0.2.5b8; http://gmt.genome.wustl.edu/packages/pindel/) and FLT3_ITD_ext (26) (version 1.1; https://github.com/ht50/FLT3_ITD_ext) were run on exon 13-15 to identify FMS-like tyrosine kinase 3 internal tandem duplication alleles. Next-generation sequencing materials are shown in Table IV.

Flow cytometry

Experimental procedure. For cell membrane antibodies, antibody was added to the specimen, followed by mixing by gentle oscillation and incubation for 15-30 min at 20˚C away from light. Red blood cell lysis reagents (1.5 ml) were added into samples, which were gently shaken and mixed evenly, and the process of lysing red blood cells lasted 10 min at 20˚C. Samples were centrifuged at 188 x g for 5 min at 20˚C, the supernatant was discarded (an appropriate amount of PBS was added before centrifugation). PBS was added for washing, and samples were mixed with gentle shaking and then centrifuged at 188 x g for 5 min at 20˚C, and the supernatant was discarded. PBS (300 μl) was added for resuspension, followed by mixing with gentle vibration and testing.

For cytoplasmic antibodies, cytoplasmic antibodies and specimens were mixed with gentle shaking, and incubated for 15-30 min at 20˚C away from light. The fixation reagent (100 μl) was added, and samples were mixed with gentle shaking and incubated for 5 min in the dark at 20˚C. Hemolysin (1.5 ml) was added, samples were mixed with gentle shaking, hemolysis was performed for 10 min at 20˚C, centrifugation was performed at 282 x g for 5 min at 20˚C and the supernatant was discarded. The permeabilization reagent (50 μl) and plasma antibody were

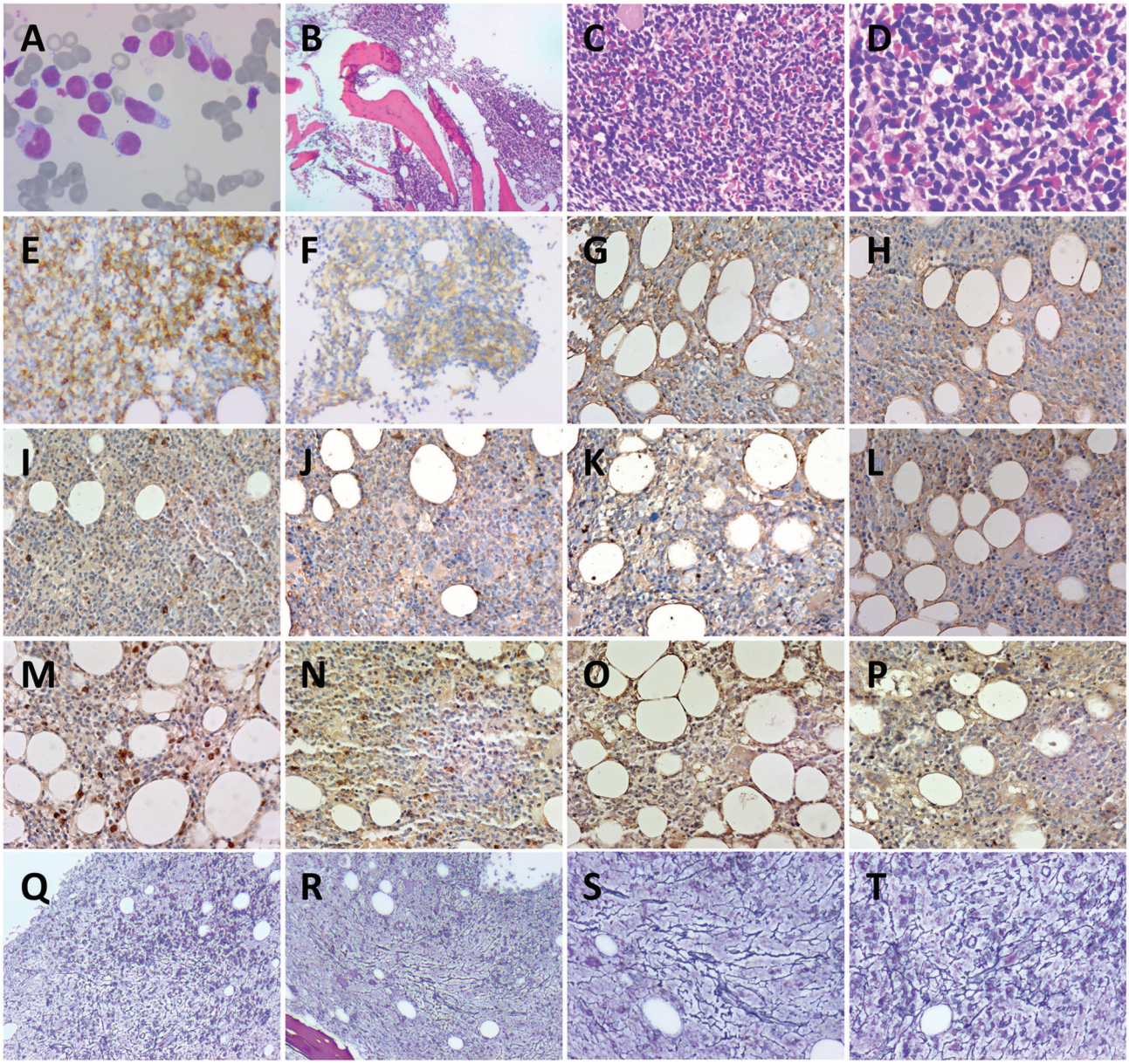

Figure 2. Bone marrow smear and pathology. (A) Wright-Giemsa staining of bone marrow smear (magnification, x1,000). Hematoxylin and eosin staining of bone marrow at (B) x40 magnification, (C) x200 magnification and (D) x400 magnification. (E) $CD56^+$ (magnification, x200), (F) $CD123^+$; (magnification, x200), (G) IL-6^- (magnification, x200), (H) IL-10^- (magnification, x200), (I) $JAK2^-$ (magnification, x200), (J) STAT3- (magnification, x200), (K) TGF-β1- (magnification, x200), (L) PDGFRA- (magnification, x200), (M) NF-$κB^+$ (magnification, x200), (N) $TET2^+$ (magnification, x200), (O) $NRAS^+$ (magnification, x200) and (P) p-ERK+ (magnification, x200) immunohistochemistry staining results. Reticular fiber staining to assess myelofibrosis-2 at (Q and R) x40 and (S and T) x200 magnification. (Q and R) and (S and T) Different positions at the same magnification. Bone marrow cells were round or sub-round. Cytoplasm was abundant and part of the cytoplasm was trailing. Nuclei were round or sub-round with rough chromatin.

added, samples were mixed with gentle shaking and incubated for 15 min in the dark at 20˚C. An appropriate amount of PBS was added for washing, samples were centrifuged at 282 x g for 5 min at 20˚C, and the supernatant was discarded. PBS (300 μl) was added for resuspension, samples were mixed with gentle shaking, and then tested.

All experimental steps of flow cytometry were performed at room temperature (~20˚C).

Reagents. Red blood cell lysis reagents for flow cytometry analysis (item no. 349202; BD Biosciences) were used. Fixation and permeation reagents were included in the BD INTRASURE KIT RUO (item no. 641776; BD Biosciences). The fluorescence reagents are shown in Table V.

Instrument and analysis. The flow cytometer used was the FACSCantoII (488/633/405 nm triple laser 8 colors) flow cytometer from BD Biosciences. Kaluza Analysis software version number 2.1.00000.20651 (Beckman Coulter, Inc.) was used. A FSC-H-Line/FSC-A-Line dual-parameter scatter was drawn to remove adherent cells. A FSC-A-Line/SSC-A-Log dual-parameter scatter was drawn to remove debris. A CD45-A-Log/SSC-A-Log dual-parameter scatter was drawn to set up a gate to circle out the nucleated cells, and to distinguish between the normal cell population and the abnormal cell population. According to the normal cell population as an internal control, whether the abnormal cells expressed the target antigen and the degree of expression were determined.

Table III. Analysis of the peripheral blood.

Parameter	On admission	Day of chemotherapy				Day after the first course of chemotherapy			
		2	5	7	9	2	3	5	6
White blood cells, 10^9/l	10.53	5.71	3.52	2.99	2.76	2.33	2.12	2.1	3.36
Neutrophils, 10^9/l	1.81	0.88	0.93	0.79	0.98	2.02	1.81	1.39	2.14
Lymphocytes, 10^9/l	7.60	4.40	2.04	1.70	1.28	0.24	0.23	0.49	1.10
Red blood cells, 10^{12}/l	3.10	2.75	2.79	2.85	3.01	3.10	3.06	3.26	2.96
Hemoglobin, g/l	91.00	79.00	80.00	81.00	85.00	92.00	89.00	94.00	86.00
Platelets, 10^9/l	70.00	44.00	91.00	114.00	112.00	104.00	73.00	17.00	8.00

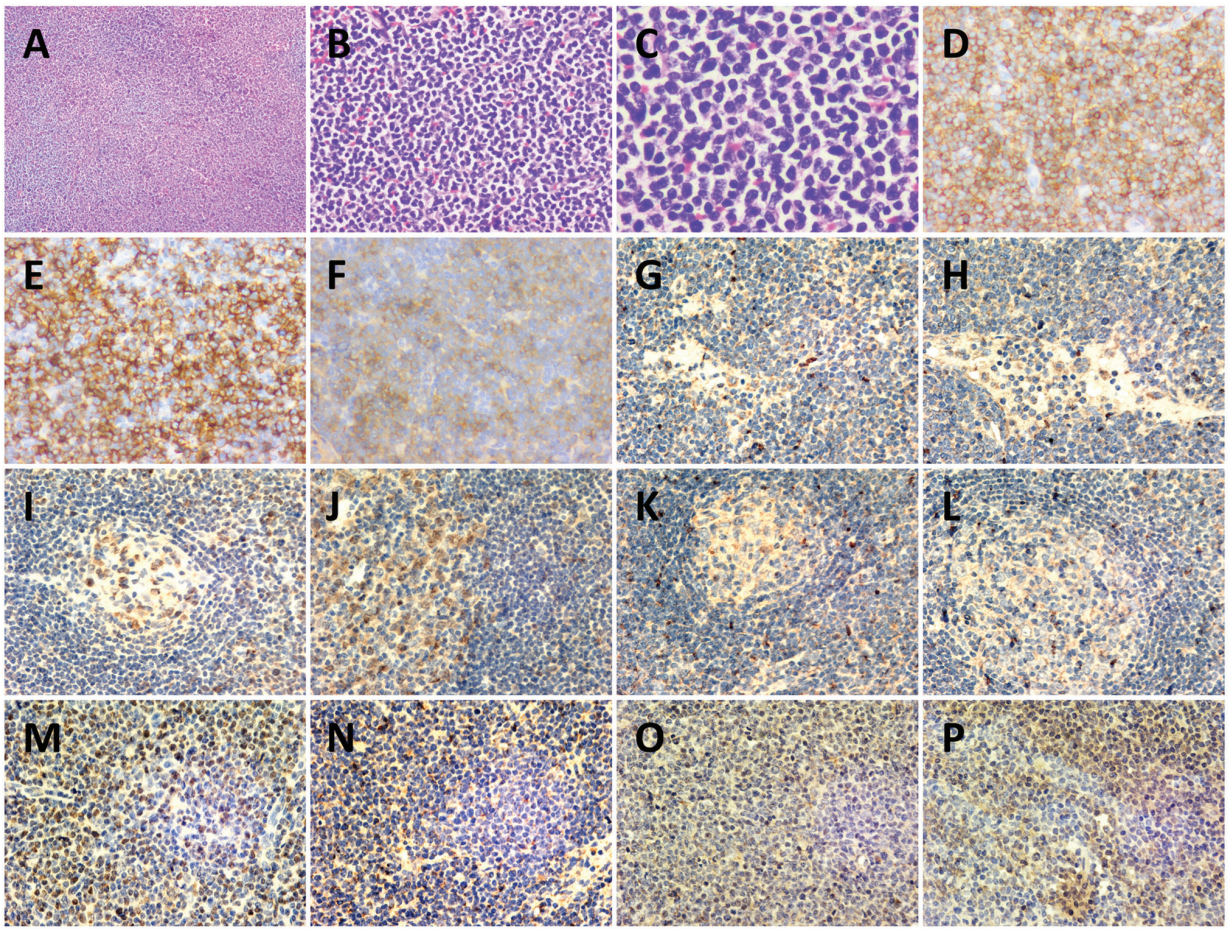

Figure 3. Histopathology of a left cervical lymph node biopsy. Hematoxylin-eosin staining of lymph node at (A) x40, (B) x200 and (C) x400 magnification. (D) $CD43^+$ (magnification, x200), (E) $CD56^+$ (magnification, x200), (F) $CD123^+$ (magnification, x200), (G) IL-6^- (magnification, x200), (H) IL-10^- (magnification, x200), (I) $JAK2^-$ (magnification, x200) (J) $STAT3^-$ (magnification, x200), (K) TGF-$\beta1^-$ (magnification, x200), (L) $PDGFRA^-$ (magnification, x200), (M) NF-κB^+ (magnification, x200), (N) $TET2^+$ (magnification, x200), (O) $NRAS^+$ (magnification, x200) and (P) p-ERK^+ (magnification, x200) immunohistochemistry staining results. The structure of the lymph node was destroyed, and atypical proliferative blast-like cells had diffusely proliferated and were mainly infiltrating the interlobular area and medullary area. Cells were medium in size with a uniform morphology, round or ovoid nucleus, fine and granular chromatin, with one or more nucleoli visible, and mitosis was common.

Immunophenotyping of the abnormal cell population was performed.

Immunohistochemistry

Reagents and instruments. Reagents and instruments used are shown in Tables VI and VII.

Methods. Bone marrow cell smear staining was performed according to the Wright-Giemsa Composite Stain Kit instructions. The smear was covered with Wright-Giemsa Stain and stained for 1-2 min at 20˚C. A light microscope was used (BX51T-PHD-J11; Olympus Corporation).

Table IV. Materials for next-generation sequencing.

Reagent name	Supplier	Step
No nuclease water	Tiangen Biotech Co., Ltd.	Overall process
Blood Genomic DNA Extraction Kit (0.1-1 ml)	Tiangen Biotech Co., Ltd.	Extraction
Illumina DNA Prep with Enrichment kits	Illumina, Inc.	Library construction
AMPure XP Beads	Beckman Coulter, Inc.	Library construction
Qubit™ dsDNA HS Assay Kits	Thermo Fisher Scientific, Inc.	Quality testing
Nextera DNA Flex Pre-Enrichment Library Prep and Enrichment Reagents 96 samples	Illumina, Inc.	Hybridization
Agilent DNF-915 Reagent Kits	Agilent Technologies, Inc.	Fragment analysis
NovaSeq6000 S1 Reagents Kit v1.5 (300 cycles)	Illumina, Inc.	Machine sequencing

Table V. Antibodies.

Antibody	Manufacturer	Product no.
CD56	Beckman Coulter, Inc.	B49189
CD303	BioLegend, Inc.	354204
CD45RA	BD Biosciences	663496
HLA-DR	BioLegend, Inc.	307618
CD36	Beckman Coulter, Inc.	IM0766U
CD2	Beckman Coulter, Inc.	A21689
CD103	Beckman Coulter, Inc.	IM1856U
CD123	BioLegend, Inc.	306010
CD7	Beijing Kuangbo Biotechnology Co., Ltd.	A6005R12
TCL-1	BioLegend, Inc.	330506
TIA-1	Beckman Coulter, Inc.	IM3293
CD4	BD Biosciences	341654
CD10	Beckman Coulter, Inc.	A07760
CD1a	BD Biosciences	560945
CD99	BD Biosciences	555689
CD33	BD Biosciences	664937
CD13	BD Biosciences	557454
TDT	Dako; Agilent Technologies, Inc	F713950
CD5	BD Biosciences	665001
CD117	BD Biosciences	664936
CD34	BioLegend, Inc.	343522
CD38	BioLegend, Inc.	303516
mCD3	BD Biosciences	663490
cCD3	BD Biosciences	558117
CD94	BD Biosciences	559876
CD8	BD Biosciences	641400
CD26	BD Biosciences	340426
CD30	Beckman Coulter, Inc.	IM2033U
CD25	BD Biosciences	560503
GranzymeB	BioLegend, Inc.	515408
Perforin	BioLegend, Inc.	308106
CD161	BioLegend, Inc.	339906

Table V. Continued.

Antibody	Manufacturer	Product no.
CD304	BioLegend, Inc.	354510
CD45RO	BD Biosciences	340438

Cytoplasmic antibodies included TCL-1, TIA-1, TDT, cCD3, GranzymeB and Perforin. Cell membranes antibodies included CD56, CD303, CD45RA, HLA-DR, CD36, CD2, CD103, CD123, CD7, CD4, CD10, CD1a, CD99, CD33, CD13,CD5, CD117, CD34, CD38, mCD3, CD94, CD8, CD26, CD30, CD25, CD161, CD304 and CD45RO. All antibodies were directly labeled antibodies and no secondary antibody was required for this experiment.

Immunohistochemistry. The protein expression levels of CD123, CD56, CD43, IL-6, IL-10, JAK2, NF-κB, TET2, TGF-β1, NRAS and p-ERK in pathological tissues were detected using immunohistochemical staining, and the results were interpreted by senior pathologists. The cell positivity rate was observed at a high magnification in five fields of view.

Fixation was performed using 4% paraformaldehyde at 20˚C for 1-3 days. For intracellular antigens or membrane proteins with an internal epitope, the permeabilization reagent was 0.1% Triton X-100. The required pathological tissue wax block was identified in the pathology specimen bank of Hebei General Hospital (Shijiazhuang, China), according to the pathology number of the patient. The wax block was cooled and fixed on the slicer. For slicing, the thickness of the tissue section was 3 μm, the cut tissue sections were spread, taken out, attached to the poly-lysine attached slides and baked at 60˚C for 12 h. The sections were sequentially immersed in xylene, 100, 95, 90, 85 and 75% ethanol, and this operation was performed in each reagent two times each for 5 min each. After the sections were removed, tap water and PBS were used to rinse the sections two times consecutively for 5 min each. The sections were incubated in 1% methanol hydrogen peroxide, placed at room temperature for 10 min, washed once with distilled water and three times with 0.1 M PBS for 5 min each. The sections were placed in 0.01 M citrate buffer (pH 6.0) and underwent microwave radiation in a microwave oven for 10 min. After the citrate buffer was reduced to

Table VI. Reagents for immunohistochemistry.

Main experimental reagents	Manufacturer	Product number
Anti-CD123 Polyclonal Antibody	OriGene Technologies, Inc.	ZM-0423
Anti-CD56 Polyclonal Antibody	OriGene Technologies, Inc.	ZM-0057
Anti-CD43 Polyclonal Antibody	OriGene Technologies, Inc.	ZM-0048
Anti-PDGFRA Polyclonal Antibody	BIOSS	bs-10989R
Anti-IL-6 Polyclonal Antibody	BIOSS	bs-4539R
Anti-IL-10 Antibody	Boster Biological Technology	BA1201-1
Anti-JAK2 Polyclonal Antibody	BIOSS	bs-0908R
Anti-NFKB P65 Polyclonal Antibody	BIOSS	bs-0465R
Anti-STAT3 Polyclonal Antibody	BIOSS	bs-1141R
Anti-TET2 Polyclonal Antibody	BIOSS	bs-9449R
Anti-TGF-β1/TGFB1 Antibody	Boster Biological Technology	BA0290
Secondary Antibody	OriGene Technologies, Inc.	Pv-6001
Wright-Giemsa Stain composite Stain kit	BIOSS	S0217
Xylene	Tianjin Yongda Chemical Reagent Co., Ltd.	YD20220904
Alcohol	Tianjin Yongda Chemical Reagent Co., Ltd.	YD20220720
Hematoxylin Staining Solution	OriGene Technologies, Inc.	ZLI-9610
Differentiation solution	Shanghai Yuanye Biotechnology Co., Ltd.	R33065
Bluing Solution	Shanghai Yuanye Biotechnology Co., Ltd.	R22272
Eosin staining solution	OriGene Technologies, Inc.	ZLI-9613
Neutral resin	OriGene Technologies, Inc.	ZLI-9555
Paraffin wax, melting point 56-58˚C	Beijing BHKT Clinical Reagent Co., Ltd.	007003

20˚C, the sections were washed three times with 0.1 M PBS for 5 min each. Drops of normal goat serum sealing solution (undiluted working solution; OriGene Technologies, Inc.) were added to the sections and the sections were left at room temperature for 20 min. Excess liquid was shaken off without washing. Primary antibodies were diluted 1:200. Pre-diluted primary antibody was added dropwise to the slices, uniformly covering the pathological tissue. The secondary antibody was ready-to-use and did not require dilution. The sections were incubated for 12 h at 4˚C, rewarmed and washed three times with 0.1 M PBS for 5 min. Biotinylated secondary antibody (IgG) was added dropwise to the slices. Slices were incubated at 37˚C for 20 min, washed three times with 0.1 M PBS for 5 min. Horseradish enzyme-labeled streptavidin working solution was added dropwise to the slices. Slices were incubated at 37˚C for 20 min and washed three times with 0.1 M PBS for 5 min. One drop each of color developer A, B and C of the DAB color development kit (cat. no. DA1016; Beijing Solarbio Science & Technology Co., Ltd.) was added to 1 ml distilled water and the liquid was mixed well, then the mixed liquid was added dropwise to the specimen and left to stand for 6 min, then the specimens were washed well with water. Cell nuclei were re-stained with hematoxylin at 20˚C for 1 min, sections were washed thoroughly with water, 1% hydrochloric acid alcohol was added for differentiation and 1% amine water was added for bluing, and sections were washed thoroughly with water, dehydrated with 70% ethanol for 5 min, 80% ethanol for 5 min, 90% ethanol for 5 min twice, 95% ethanol for 5 min twice, 100% ethanol for 5 min twice, cleared with xylene for 5 min twice, sealed with neutral resin and air-dried. For light microscopy observation, five high magnification fields of view (magnification, x400) were selected, the positive cells were counted, the average of the five fields of view was taken as the average positive rate and images were captured. Myelofibrosis was graded according to the World Health Organization (2016) myelofibrosis grading criteria (21).

Silver nitrate methods. Fixation was performed using 4% paraformaldehyde at 20˚C for 1-3 days. The thickness of the tissue section was 3 μm. Sections were dewaxed to water and washed with distilled water. Sections were immersed in 1% silver nitrate solution at 20˚C for 30-60 min. After the slice was removed, the excess silver nitrate solution on the edge of the slide was absorbed using filter paper, and the sections were washed with 50% ethanol at 20˚C for 5-10 sec, and then with distilled water. The sections were placed in aqueous gold chloride solution at 20˚C for 5 min until the yellowish brown color was removed, and then the staining was intensified by dropping aniline oil ethanol on the sections at 20˚C for ~15 sec. After rinsing the sections with running water, the sections were treated with 2% sodium thiosulfate solution at 20˚C for 2 min. After rinsing the sections in running water, the sections were dehydrated, cleared with xylene and sealed with neutral resin. A CMOS light microscope (DP22; Olympus Corporation) was used, as shown in Table VII.

Discussion

BPDCN is an aggressive hematopoietic neoplasm derived from plasmacytoid dendritic cells and was first reported in 1994 (27). BPDCN mainly occurs in elderly patients aged 60-70 years

Table VII. Instruments for immunohistochemistry.

Main experimental instruments	Manufacturer	Product model
Microscope	Olympus Corporation	BX51T-PHD-J11
CMOS	Olympus Corporation	DP22
Multi-functional True Color Cell Image Analysis Management System	Media Cybernetics, Inc.	Image-Pro Plus 6.0
Paraffin Slicer	Leica Microsystems GmbH	RM2015
Centrifuge	Eppendorf SE	5430
Cryogenic refrigerator	Sanyo	MDF-382E
Pipette	Eppendorf SE	3123000
Constant temperature water bath	Taicang HuadaExperimental Instrument Technology Co., Ltd. (Huamei Biochemical Instrument Factory)	DSHZ-300

with a high male proportion. BPDCN most commonly presents with skin lesions, and bone marrow involvement is also frequent. The clinical presentation varies widely, and there can be either single or multiple skin lesions. Skin lesions appear as brown or purplish-red rashes, plaques or nodules. This is often associated with involvement of peripheral blood, bone marrow and lymph nodes, which usually show diffuse proliferation or infiltration of abnormal matricellular-like cells (28). Tissue biopsies of the bone marrow, lymph nodes and skin of the patient in the present case report showed abnormal blastocyte-like cells. Only one case report has been reported that found conversion of PMF to BPDCN (20), but there is no relevant literature on MF secondary to BPDCN. Therefore, it is rare for BPDCN to occur simultaneously with MF. MF is a Philadelphia chromosome-negative MPN with increased deposition of collagen fibers in bone marrow hematopoietic tissue under certain conditions, causing abnormal hematopoiesis. The pathogenesis of MPN is unclear and is mainly associated with three clonal mutations, JAK2, CALR and MPL, and can lead to constitutive activation of the JAK/STAT signaling pathway. Conversely, triple-negative PMF is not associated with mutations in the JAK2, CALR and MPL genes, but >50% of patients with MF have with mutations in the TET2, additional sex combs like 1-transcriptional regulator and DNA (cytosine-5-)-methyltransferase 3α genes (29). A case of follicular lymphoma with MF was previously diagnosed at Hebei General Hospital (Shijiazhuang, China). Several cytokines were detected, such as basic fibroblast growth factor, TNF-α, TGF-β, PDGF, IL-1β, IL-2, IL-6 and IL-10, which promoted the development of non-Hodgkin's lymphoma with MF. Moreover, the results indicated that activation of the JAK/STAT pathway may be a common mechanism in the development of B-cell non-Hodgkin's lymphoma and secondary MF (30).

The bone marrow biopsy pathology in the present case revealed that reticular fiber staining was grade 2, and next-generation sequencing of the peripheral blood demonstrated mutations in the PDGFRA, TET2 and NRAS genes, but no mutations in JAK2, STAT, CALR or MPL. According to the diagnostic criteria for autoimmune MF (AIMF), the presence of positive autoantibodies is required for AIMF, and the negative autoantibodies in the present case, combined with the absence of previous autoimmune disease (AIMF is usually associated with a well-defined autoimmune disease), ruled out AIMF (31). Cytokine assays of the peripheral blood showed elevated levels of IL-6 and IL-10. However, immunohistochemical examination of bone marrow and lymph nodes revealed the expression of only TET2 and NF-κB, with a negative result for the expression of PDGFRA, IL-6, IL-10, JAK2, STAT3 and TGF-β1. These results indicate that the occurrence of MF in the present case may not have been caused by activation of the classical JAK/STAT pathway. Similar to these results, Beird *et al* (32) reported that JAK/STAT signaling in BPDCN, and the levels of the upstream and downstream molecular serum proteins (colony stimulating factor 3 receptor, STAT3 and STAT5B) in this pathway were low, which may be related to the high level of IL-3Rα in BPDCN, which inhibits IL-3/STAT3 signal transduction.

MF may occur before and/or after the development of other hematological malignancies (30,33,34). Although the patient in the present case did not have mutations in JAK2, CALR or MPL, another clonal proliferative marker, TET2, was present. When MF and other hematological malignancies occur together, it is difficult to determine whether the disorder is triple-negative primary MF or secondary MF (30,34-37). In the present case, we hypothesize that secondary MF was more likely and that the primary BPDCN had invaded the bone marrow and caused secondary MF.

The mechanism of BPDCN combined with MF was further assessed. Somatic point mutations of TET2 and NRAS are often found in patients with BPDCN (3). TET2 encodes an enzyme that catalyzes 5-methyl cytosine oxidation to 5-hydroxymethylcytosine. When TET2 is mutated, it leads to loss of function of this enzyme and DNA hypermethylation, which subsequently amplifies precancerous clones of bone marrow and abnormal hematopoiesis, driving MPN development (38-41). Ostrander *et al* (42) reported that the TET2 deletion mutation increases dendritic cell production, increases hematopoietic stem cell self-renewal and polarizes toward the myeloid lineage. NRAS is a member of the RAS family, and mutations in NRAS facilitate GTP binding of RAS, thereby promoting constitutive activation of the RAS-RAF-MEK-ERK/MAPK signaling pathway and causing abnormal proliferation of myeloid

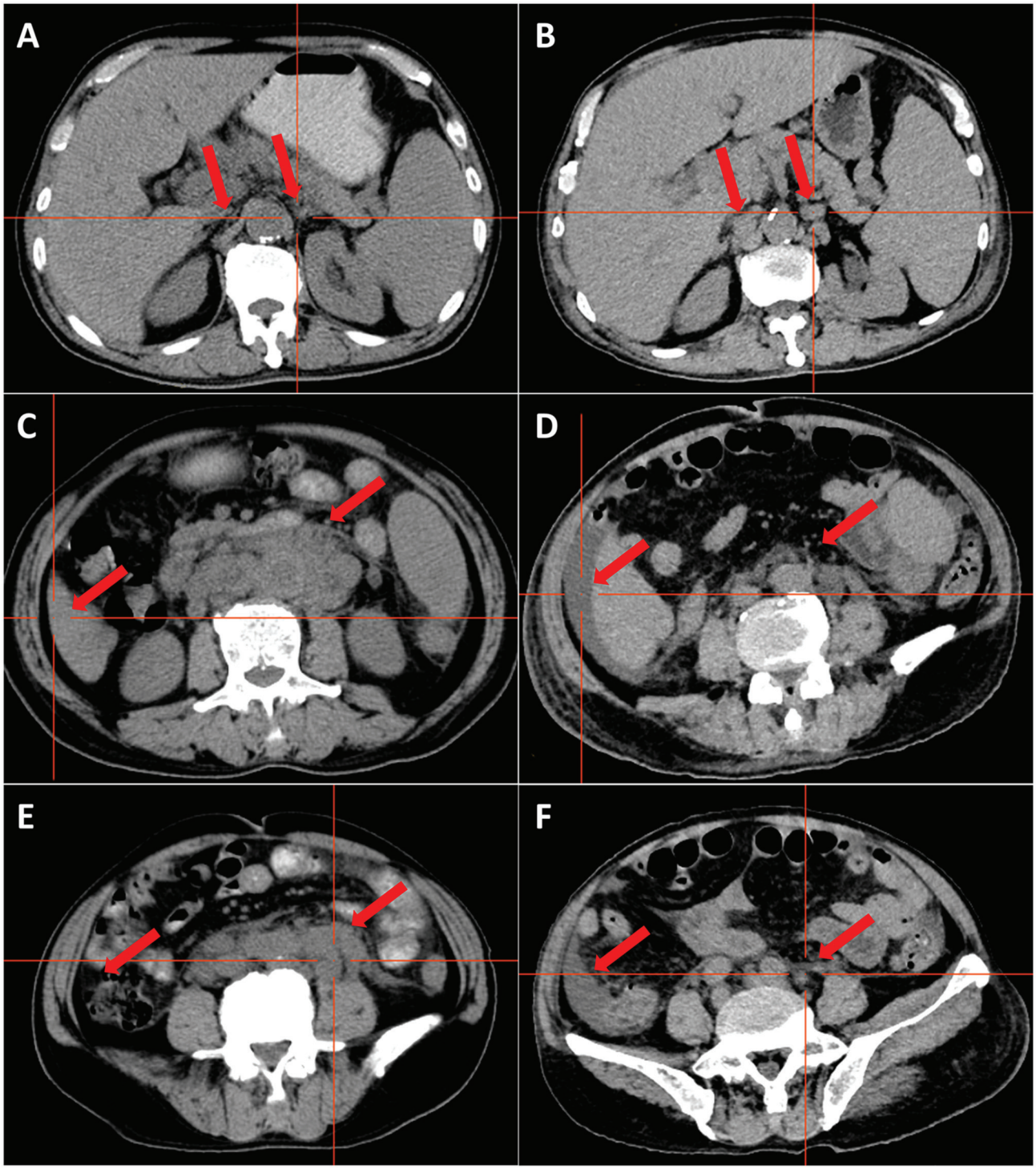

Figure 4. Computed tomography images at first vs. second admission. Lymph nodes behind the pancreas (A) before and (B) after treatment, highlighted by red arrows; no lymph nodes were seen on either side of the abdominal aorta before treatment, and ~6 lymph nodes with a maximum size of 16x8 mm appeared on both sides of the abdominal aorta after treatment. Lymph nodes around the abdominal aorta and retroperitoneum (C) before and (D) after treatment, highlighted by red arrows. Before treatment, there were numerous enlarged lymph nodes adjacent to the retroperitoneal abdominal aorta, some of which were fused to each other, making it difficult to determine the exact number of lymph nodes, the largest of which was 30x20 mm in size. After treatment, the lymph nodes were significantly reduced and some of them had subsided. Ascites (E) before and (F) after treatment, highlighted by red arrows. No ascites was seen before the treatment. Ascites appeared after the treatment.

cells (41,43). This may be involved in the occurrence of MF. As specimens from the patient in the present case were limited, only the expression of NRAS and p-ERK was assessed, and it was found that both NRAS and p-ERK were expressed in the bone marrow and lymph nodes of the patient. This indicates that the mutations in TET2 and NRAS may be the bridge between BPDCN and MF, but whether RAS-related pathways are involved requires further experiments for verification.

Although mutations in TET2 and NRAS may be the potential pathological associating factors between BPDCN and MF,

it may also be a unique coincidence in the patient in the present case. In addition to TET2 and NRAS, other mutated genes in the patient appeared to be indirectly associated with the development of BPDCN or MF. It has been reported that loss of function in DIS3 increases the RAS protein level in multiple myeloma cells, which promotes the development of cancer cells (44). CSMD1 is a tumor suppressor gene, and dysregulation of CSMD1 can drive the NF-κB pathway and promote tumor progression (45). B-cell lymphoma 6 corepressor (BCOR) mutations occur after mutations affecting splicing mechanisms or epigenetically regulated genes (46). Patients with adult acute myeloid leukemia with BCOR mutations are predicted to have a complete response to venetoclax plus hypomethylating agents (47), and BCOR has been reported to respond better to hypomethylating drugs when it is co-mutated with other genes that regulate epigenetic inheritance, such as TET2 (48). PDGFRA mutations or rearrangements serve an important role in the development of hypereosinophilic syndrome and its mutation sites (H650Q, N659S, R748G and Y849S). Additionally, FIP1L1-PDGFRA has been reported to induce the activation of STAT5 and sensitivity to imatinib (49). Abdulbaki *et al* (50) reported a case of BPDCN presenting with a PDGFRA mutation and suggested the possibility of tyrosine kinase inhibitors for the treatment of BPDCN, but further studies are lacking. Overall, all of these mutations may be indirectly associated with the development of BPDCN or MF, and thus more future cases are needed for further study.

Personalized treatment based on the immune phenotype and mutation profile of a patient is important. CD123 is a plasmacytoid dendritic cell-specific surface marker that is prevalent in BPDCN, and tagraxofusp targets CD123. Macrophage dendritic cell progenitors are common precursor cells of plasmacytoid dendritic cells and monocytes (51), whereas tumorigenic monocyte-derived fibroblasts contribute to myeloid cell fibrosis (52). A small number of circulating cells have been reported to express CD123 in patients with MF (53), which can be targeted to treat BPDCN in conjunction with MF. Clinical studies of tagraxofusp monotherapy for MF are currently underway (trial registration nos. NCT0226825 and NCT05233618). Additionally, clinicians can target therapy in accordance with other specific immunophenotypes of BPDCN, such as targeting CD303 (litifilimab) (54), TCF4 (bromodomain and extra-terminal domain inhibitors act by inhibiting TCF4) (55) and BCL2 (venetoclax) (56). BPDCN is closely related to DNA hypermethylation (57). In the present case, the patient presented with a TET2 mutation and was treated with the DNA methyltransferase inhibitor, azacytidine, in combination with venetoclax. Certain cases of BPDCN have been treated with azacitidine in combination with venetoclax and it was well tolerated (58,59). Moreover, azacitidine combined with tagraxofusp has been reported to be effective for BPDCN treatment, with azacitidine restoring sensitivity to tagraxofusp by restoring diphthamide biosynthesis protein 1 expression (60). In terms of the NRAS mutation in the patient in the present case, an RAF or an ERK inhibitor may have been appropriate for use (61).

Furthermore, several retrospective clinical studies have reported that achieving complete remission after first-line therapy is the primary condition for long-term survival of patients with BPDCN and that survival is prolonged by allogeneic hematopoietic cell transplantation during the first complete remission (4). Patients with MF have reduced blood cell counts, and in the context of malignancy, patients with MF are more (62) likely to have myelosuppression after chemotherapy (63,64). The patient in the present case had induced myelosuppression after chemotherapy with poor efficacy, along with a severe infection, which finally led to the poor outcome. Therefore, BPDCN combined with MF may represent a poor prognosis with a limited therapeutic effect. For such patients, physicians need to be particularly mindful of infections associated with myelosuppression during chemotherapy. While preventing or fighting infection, the selection of reasonable chemotherapeutic drugs and doses should be focused on.

In conclusion, patients with BPDCN and MF have a poor prognosis, and mutations in TET2 and NRAS may be the bridge between the two conditions. The findings of the present case indicate the need for increased awareness of BPDCN among clinicians in order to reduce misdiagnosis and improve the prognosis of patients with BPDCN, to ensure appropriate and individualized chemotherapeutic agents for the treatment of patients with BPDCN and MF, and to increase awareness of potentially fatal infections that may occur after myelosuppression during chemotherapy.

Acknowledgements

Not applicable.

Funding

The present study was financially supported by the Department of Science and Technology of Hebei Province Plan Project (Priority Research and Development Project; grant no. 18277720D).

Availability of data and materials

The datasets generated and/or analyzed during the current study are available in the National Center for Biotechnology Information database, https://www.ncbi.nlm.nih.gov/sra/SRR26895553.

Authors' contributions

YL made decisions regarding patient treatment. FL and YL were accountable for all aspects of the work and contributed to the analysis and interpretation of the data, and also contributed to manuscript drafting and critical revisions of the intellectual content. BL and JL analyzed and interpreted the data, and contributed to the Discussion section. FL, BL, JL and YL confirm the authenticity of all the raw data. All authors have read and approved the final manuscript.

Ethics approval and consent to participate

Not applicable.

Patient consent for publication

Written informed consent was obtained from the patient for the publication of anonymized data and any accompanying images.

Competing interests

The authors declare that they have no competing interests.

References

1. Guru Murthy GS, Pemmaraju N and Atallah E: Epidemiology and survival of blastic plasmacytoid dendritic cell neoplasm. Leuk Res 73: 21-23, 2018.
2. Pagano L, Valentini CG, Pulsoni A, Fisogni S, Carluccio P, Mannelli F, Lunghi M, Pica G, Onida F, Cattaneo C, *et al*: Blastic plasmacytoid dendritic cell neoplasm with leukemic presentation: An Italian multicenter study. Haematologica 98: 239-246, 2013.
3. Jain A and Sweet K: Blastic plasmacytoid dendritic cell neoplasm. J Natl Compr Canc Netw 21: 515-521, 2023.
4. Garnache-Ottou F, Vidal C, Biichlé S, Renosi F, Poret E, Pagadoy M, Desmarets M, Roggy A, Seilles E, Soret L, *et al*: How should we diagnose and treat blastic plasmacytoid dendritic cell neoplasm patients? Blood Adv 3: 4238-4251, 2019.
5. Khoury JD, Solary E, Abla O, Akkari Y, Alaggio R, Apperley JF, Bejar R, Berti E, Busque L, Chan JKC, *et al*: The 5th edition of the World Health Organization classification of haematolymphoid tumours: Myeloid and histiocytic/dendritic neoplasms. Leukemia 36: 1703-1719, 2022.
6. Facchetti F, Cigognetti M, Fisogni S, Rossi G, Lonardi S and Vermi W: Neoplasms derived from plasmacytoid dendritic cells. Mod Pathol 29: 98-111, 2016.
7. Pemmaraju N, Kantarjian H, Sweet K, Wang E, Senapati J, Wilson NR, Konopleva M, Frankel AE, Gupta V, Mesa R, *et al*: North American blastic plasmacytoid dendritic cell neoplasm consortium: Position on standards of care and areas of need. Blood 141: 567-578, 2023.
8. Yun S, Chan O, Kerr D, Vincelette ND, Idrees A, Mo Q, Sweet K, Lancet JE, Kharfan-Dabaja MA, Zhang L and Sokol L: Survival outcomes in blastic plasmacytoid dendritic cell neoplasm by first-line treatment and stem cell transplant. Blood Adv 4: 3435-3442, 2020.
9. Taylor J, Haddadin M, Upadhyay VA, Grussie E, Mehta-Shah N, Brunner AM, Louissaint A Jr, Lovitch SB, Dogan A, Fathi AT, *et al*: Multicenter analysis of outcomes in blastic plasmacytoid dendritic cell neoplasm offers a pretargeted therapy benchmark. Blood 134: 678-687, 2019.
10. Huang L and Wang F: Primary blastic plasmacytoid dendritic cell neoplasm: A US population-based study. Front Oncol 13: 1178147, 2023.
11. Murthy HS, Zhang MJ, Chen K, Ahmed S, Deotare U, Ganguly S, Kansagra A, Michelis FV, Nishihori T, Patnaik M, *et al*: Allogeneic hematopoietic cell transplantation for blastic plasmacytoid dendritic cell neoplasm: A CIBMTR analysis. Blood Adv 7: 7007-7016, 2023.
12. Tefferi A: Primary myelofibrosis: 2023 Update on diagnosis, risk-stratification, and management. Am J Hematol 98: 801-821, 2023.
13. Titmarsh GJ, Duncombe AS, McMullin MF, O'Rorke M, Mesa R, De Vocht F, Horan S, Fritschi L, Clarke M and Anderson LA: How common are myeloproliferative neoplasms? A systematic review and meta-analysis. Am J Hematol 89: 581-587, 2014.
14. Cervantes F, Dupriez B, Pereira A, Passamonti F, Reilly JT, Morra E, Vannucchi AM, Mesa RA, Demory JL, Barosi G, *et al*: New prognostic scoring system for primary myelofibrosis based on a study of the international working group for myelofibrosis research and treatment. Blood 113: 2895-2901, 2009.
15. McLornan DP, Psaila B, Ewing J, Innes A, Arami S, Brady J, Butt NM, Cargo C, Cross NCP, Francis S, *et al*: The management of myelofibrosis: A British society for haematology guideline. Br J Haematol 204: 136-150, 2024.
16. Tashi T, Yu J, Pandya S, Dieyi C, Scherber R and Parasuraman S: Trends in overall mortality among US veterans with primary myelofibrosis. BMC Cancer 23: 48, 2023.
17. Thiele J and Kvasnicka HM: Myelofibrosis-what's in a name? Consensus on definition and EUMNET grading. Pathobiology 74: 89-96, 2007.
18. Wang N, Xu H, Li Q, Fang X, Liu J, Sui X, Zhang L, Jiang Y and Wang X: Patients of myelodysplastic syndrome with mild/moderate myelofibrosis and a monosomal karyotype are independently associated with an adverse prognosis: Long-term follow-up data. Cancer Manag Res 12: 5881-5891, 2020.
19. Shehata M, Schwarzmeier JD, Hilgarth M, Hubmann R, Duechler M and Gisslinger H: TGF-beta1 induces bone marrow reticulin fibrosis in hairy cell leukemia. J Clin Invest 113: 676-685, 2004.
20. Shenjere P, Chasty R, Chaturvedi A, Dennis MW, Ong A, Wiseman DH and Menasce LP: E-cadherin expression in blastic plasmacytoid dendritic cell neoplasms: An unrecognized finding and potential diagnostic pitfall. Int J Surg Pathol 29: 289-293, 2021.
21. Arber DA, Orazi A, Hasserjian R, Thiele J, Borowitz MJ, Le Beau MM, Bloomfield CD, Cazzola M and Vardiman JW: The 2016 revision to the World Health Organization classification of myeloid neoplasms and acute leukemia. Blood 127: 2391-2405, 2016.
22. Chen S, Zhou Y, Chen Y and Gu J: Fastp: An ultra-fast all-in-one fastq preprocessor. Bioinformatics 34: i884-i890, 2018.
23. Thorvaldsdóttir H, Robinson JT and Mesirov JP: Integrative genomics viewer (IGV): High-performance genomics data visualization and exploration. Brief Bioinform 14: 178-192, 2013.
24. Talevich E, Shain AH, Botton T and Bastian BC: CNVkit: Genome-wide copy number detection and visualization from targeted DNA sequencing. PLoS Comput Biol 12: e1004873, 2016.
25. Ye K, Guo L, Yang X, Lamijer EW, Raine K and Ning Z: Split-read indel and structural variant calling using pindel. Methods Mol Biol 1833: 95-105, 2018.
26. Tung JK, Suarez CJ, Chiang T, Zehnder JL and Stehr H: Accurate detection and quantification of FLT3 internal tandem duplications in clinical hybrid capture next-generation sequencing data. J Mol Diagn 23: 1404-1413, 2021.
27. Adachi M, Maeda K, Takekawa M, Hinoda Y, Imai K, Sugiyama S and Yachi A: High expression of CD56 (N-CAM) in a patient with cutaneous CD4-positive lymphoma. Am J Hematol 47: 278-282, 1994.
28. Julia F, Dalle S, Duru G, Balme B, Vergier B, Ortonne N, Vignon-Pennamen MD, Costes-Martineau V, Lamant L, Dalac S, *et al*: Blastic plasmacytoid dendritic cell neoplasms: Clinico-immunohistochemical correlations in a series of 91 patients. Am J Surg Pathol 38: 673-680, 2014.
29. Arber DA, Orazi A, Hasserjian RP, Borowitz MJ, Calvo KR, Kvasnicka HM, Wang SA, Bagg A, Barbui T, Branford S, *et al*: International consensus classification of myeloid neoplasms and acute leukemias: Integrating morphologic, clinical, and genomic data. Blood 140: 1200-1228, 2022.
30. Kong LZ, Li J, Wang RC, Kang L, Wei Q and Li Y: Simultaneous follicular lymphoma and myelofibrosis: Report of a case with review of the literature. Onco Targets Ther 14: 4551-4559, 2021.
31. Amel Riazat-Kesh YJR, Maraveyas A, Martin L and Tremblay D: An overlooked mimic? Autoimmune myelofibrosis-A scoping review of the literature. Eur J Haematol 111: 706-714, 2023.
32. Beird HC, Khan M, Wang F, Alfayez M, Cai T, Zhao L, Khoury J, Futreal PA, Konopleva M and Pemmaraju N: Features of non-activation dendritic state and immune deficiency in blastic plasmacytoid dendritic cell neoplasm (BPDCN). Blood Cancer J 9: 99, 2019.
33. Tabata R, Tabata C, Nagai T and Yasumizu R: Follicular lymphoma with prominent fibrosis complicated by peripheral eosinophilia. Ann Hematol 91: 965-967, 2012.
34. Scherber RM and Mesa RA: Managing myelofibrosis (MF) that 'blasts' through: Advancements in the treatment of relapsed/refractory and blast-phase MF. Hematology Am Soc Hematol Educ Program 2018: 118-126, 2018.
35. Okabe S, Miyazawa K, Iguchi T, Sumi M, Takaku T, Ito Y, Ito Y, Kimura Y, Serizawa H, Mukai K and Ohyashiki K: Peripheral T-cell lymphoma together with myelofibrosis with elevated plasma transforming growth factor-beta1. Leuk Lymphoma 46: 599-602, 2005.
36. Tsutsui M, Yasuda H, Ota Y and Komatsu N: Splenic marginal zone lymphoma with prominent myelofibrosis mimicking triple-negative primary myelofibrosis. Case Rep Oncol 12: 834-837, 2019.
37. Matsunaga T, Takemoto N, Miyajima N, Okuda T, Nagashima H, Sato T, Terui T, Sasaki H, Ohmi N, Hirayama Y, *et al*: Splenic marginal zone lymphoma presenting as myelofibrosis associated with bone marrow involvement of lymphoma cells which secrete a large amount of TGF-beta. Ann Hematol 83: 322-325, 2004.
38. Nakajima H and Kunimoto H: TET2 as an epigenetic master regulator for normal and malignant hematopoiesis. Cancer Sci 105: 1093-1099, 2014.

39. Abdel-Wahab O, Mullally A, Hedvat C, Garcia-Manero G, Patel J, Wadleigh M, Malinge S, Yao J, Kilpivaara O, Bhat R, *et al*: Genetic characterization of TET1, TET2, and TET3 alterations in myeloid malignancies. Blood 114: 144-147, 2009.
40. Delhommeau F, Dupont S, Della Valle V, James C, Trannoy S, Massé A, Kosmider O, Le Couedic JP, Robert F, Alberdi A, *et al*: Mutation in Tet2 in myeloid cancers. N Eng J Med 360: 2289-2301, 2009.
41. Vainchenker W and Kralovics R: Genetic basis and molecular pathophysiology of classical myeloproliferative neoplasms. Blood 129: 667-679, 2017.
42. Ostrander EL, Kramer AC, Mallaney C, Celik H, Koh WK, Fairchild J, Haussler E, Zhang CRC and Challen GA: Divergent effects of Dnmt3a and Tet2 mutations on hematopoietic progenitor cell fitness. Stem Cell Reports 14: 551-560, 2020.
43. Schubbert S, Shannon K and Bollag G: Hyperactive Ras in developmental disorders and cancer. Nat Rev Cancer 7: 295-308, 2007.
44. Ohguchi Y and Ohguchi H: Dis3: The enigmatic gene in multiple myeloma. Int J Mol Sci 24: 4079, 2023.
45. Chen XL, Hong LL, Wang KL, Liu X, Wang JL, Lei L, Xu ZY, Cheng XD and Ling ZQ: Deregulation of CSMD1 targeted by microRNA-10b drives gastric cancer progression through the NF-κB pathway. Int J Biol Sci 15: 2075-2086, 2019.
46. Damm F, Chesnais V, Nagata Y, Yoshida K, Scourzic L, Okuno Y, Itzykson R, Sanada M, Shiraishi Y, Gelsi-Boyer V, *et al*: BCOR and BCORL1 mutations in myelodysplastic syndromes and related disorders. Blood 122: 3169-3177, 2013.
47. Sportoletti P, Sorcini D and Falini B: BCOR gene alterations in hematologic diseases. Blood 138: 2455-2468, 2021.
48. Badaat I, Mirza S, Padron E, Sallman D, Komrokji R, Song J and Hussaini MO: Concurrent mutations in other epigenetic modulators portend better prognosis in BCOR-mutated myelodysplastic syndrome. J Clin Pathol 73: 209-212, 2020.
49. Elling C, Erben P, Walz C, Frickenhaus M, Schemionek M, Stehling M, Serve H, Cross NC, Hochhaus A, Hofmann WK, *et al*: Novel imatinib-sensitive PDGFRA-activating point mutations in hypereosinophilic syndrome induce growth factor independence and leukemia-like disease. Blood 117: 2935-2943, 2011.
50. Abdulbaki R, DeRosa PA, Mobarek D, Liu ML and Nava VE: Novel PDGFRA mutation in blastic plasmacytoid dendritic cell neoplasm; possible therapeutic implications. Br J Haematol 197: 8, 2022.
51. Collin M and Bigley V: Human dendritic cell subsets: An update. Immunology 154: 3-20, 2018.
52. Verstovsek S, Manshouri T, Pilling D, Bueso-Ramos CE, Newberry KJ, Prijic S, Knez L, Bozinovic K, Harris DM, Spaeth EL, *et al*: Role of neoplastic monocyte-derived fibrocytes in primary myelofibrosis. J Exp Med 213: 1723-1740, 2016.
53. Tremblay D and Mascarenhas J: Next generation therapeutics for the treatment of myelofibrosis. Cells 10: 1034, 2021.
54. Werth VP, Furie RA, Romero-Diaz J, Navarra S, Kalunian K, van Vollenhoven RF, Nyberg F, Kaffenberger BH, Sheikh SZ, Radunovic G, *et al*: Trial of anti-BDCA2 antibody litifilimab for cutaneous lupus erythematosus. N Engl J Med 387: 321-331, 2022.
55. Ceribelli M, Hou ZE, Kelly PN, Huang DW, Wright G, Ganapathi K, Evbuomwan MO, Pittaluga S, Shaffer AL, Marcucci G, *et al*: A druggable TCF4- and BRD4-dependent transcriptional network sustains malignancy in blastic plasmacytoid dendritic cell neoplasm. Cancer Cell 30: 764-778, 2016.
56. Montero J, Stephansky J, Cai T, Griffin GK, Cabal-Hierro L, Togami K, Hogdal LJ, Galinsky I, Morgan EA, Aster JC, *et al*: Blastic Plasmacytoid dendritic cell neoplasm is dependent on BCL2 and sensitive to venetoclax. Cancer Discov 7: 156-164, 2017.
57. Sapienza MR, Abate F, Melle F, Orecchioni S, Fuligni F, Etebari M, Tabanelli V, Laginestra MA, Pileri A, Motta G, *et al*: Blastic plasmacytoid dendritic cell neoplasm: Genomics mark epigenetic dysregulation as a primary therapeutic target. Haematologica 104: 729-737, 2019.
58. Azad F, Zhang J, Miranda CJ and Gravina M: Venetoclax and Azacitidine in the treatment of blastic plasmacytoid dendritic cell neoplasm refractory to conventional therapy. Cureus 14: e33109, 2022.
59. Samhouri Y, Ursu S, Dutton N, Tanvi V and Fazal S: Tagraxofusp followed by combined azacitidine and venetoclax in blastic plasmacytoid dendritic cell neoplasm: A case report and literature review. J Oncol Pharm Pract 27: 990-995, 2021.
60. Togami K, Pastika T, Stephansky J, Ghandi M, Christie AL, Jones KL, Johnson CA, Lindsay RW, Brooks CL, Letai A, *et al*: DNA methyltransferase inhibition overcomes diphthamide pathway deficiencies underlying CD123-targeted treatment resistance. J Clin Invest 129: 5005-5019, 2019.
61. Moore AR, Rosenberg SC, McCormick F and Malek S: RAS-targeted therapies: Is the undruggable drugged? Nat Rev Drug Discov 19: 533-552, 2020.
62. Lyman GH, Poniewierski MS and Culakova E: Risk of chemotherapy-induced neutropenic complications when treating patients with non-Hodgkin lymphoma. Expert Opin Drug Saf 15: 483-492, 2016.
63. Dinan MA, Hirsch BR and Lyman GH: Management of chemotherapy-induced neutropenia: Measuring quality, cost, and value. J Natl Compr Canc Netw 13: e1-e7, 2015.
64. Epstein RS, Aapro MS, Basu Roy UK, Salimi T, Krenitsky J, Leone-Perkins ML, Girman C, Schlusser C and Crawford J: Patient burden and real-world management of chemotherapy-induced myelosuppression: Results from an online survey of patients with solid tumors. Adv Ther 37: 3606-3618, 2020.